

SUITABILITY OF A COAL-DERIVED CARBON-BASED FOAM FOR USE IN THERMAL PROTECTION SYSTEMS OF COMMON AERO VEHICLES

M. Grujicic^{1*}, C. L. Zhao¹, S. B. Biggers¹, J. M. Kennedy¹ and D. R. Morgan²

¹*Department of Mechanical Engineering Program in Materials Science and Engineering Clemson University, Clemson SC 29634*

²*Touchstone Research Laboratory, Inc. Triadelphia, West Virginia 26059*

Received 17 December 2005; accepted 1 March 2006

Abstract— Common Aero Vehicles (CAVs) are relatively small-size, un-powered, self-maneuvering vehicles equipped with a variety of weapons and launched from space. One of the major obstacles hampering a full the realization of the CAV concept is a present lack of lightweight, high-temperature insulation materials which can be used for construction of the CAV's thermal protection system (TPS). A computational analysis is utilized in the present work to examine the suitability of a carbon-based, coal-derived foam for the TPS applications in the CAVs. Toward that end, a model is developed for the high-temperature effective thermal conductivity of foam-like materials. In addition, an insulation sizing procedure is devised to determine the minimum insulation thickness needed for thermal protection of the vehicle structure at different sections of a CAV. It is found that the carbon-based foam material in question can be considered as a suitable TPS insulation material at the leeward side and at selected portions of the windward side of a CAV (specifically the portions which are further away from the vehicle nose).

Keywords: Thermal Protection System, Porous Materials, Carbon Foams

NOMENCLATURE

a	-	Foam ligament radius (m)
C	-	Constant
C_1	-	Constant (Wm^2)
C_2	-	Constant (mK)
C_P	-	Specific heat ($J/kg\cdot K$)
d	-	Dimensionless foam ligament radius
d_g	-	Gas collision diameter (m)
E	-	Young's Modulus (Pa)
E_{bl}	-	Spectral emissive power of a black body (W/m^3)

* E-mail: mica.grujicic@ces.clemson.edu

Tel: (864) 656-5639, Fax: (864) 656-4435

E_b	-	Total emissive power of a black body (W/m^2)
e	-	Dimensionless cubic node length
h	-	Thickness (m)
K_B	-	Boltzmann's constant (J/K)
Kn	-	Knudsen number
K_R	-	Rosseland mean extinction coefficient
K_I	-	Spectral extinction coefficient
k	-	Thermal conductivity ($\text{W}/\text{m}\cdot\text{K}$)
L	-	Thickness (m)
n	-	Constant
P	-	Pressure (Pa)
Pr	-	Prandtl number
q	-	Heat flux (W/m^2)
R	-	Simplification quantity ($\text{m}\cdot\text{K}/\text{W}$)
r	-	Cubic node length (m)
T	-	Temperature (K)
t	-	Time (s)
V	-	Volume (m^3)
x	-	Spatial coordinate (m)
\mathbf{a}	-	Thermal accommodation factor
\mathbf{g}	-	Specific heat ratio
\mathbf{d}	-	Characteristic length scale for gas molecules in the porous medium (m)
\mathbf{e}	-	Porosity
\mathbf{h}	-	Emissivity
\mathbf{r}	-	Density (kg/m^3)
\mathbf{l}	-	Photon wave length (m)
\mathbf{s}	-	Stefan-Boltzmann constant ($\text{W}/\text{m}^2\cdot\text{K}^4$)
F	-	Parameter of the gas-phase regime
$?$	-	Parameter of the gas-phase regime

Subscripts

A	-	Unit cell layer
$aero$	-	Aerodynamic quantity
atm	-	Atmospheric-pressure based quantity
B	-	Unit cell layer
C	-	Unit cell layer
D	-	Unit cell layer
dyn	-	Dynamic-pressure based quantity
eff	-	Effective quantity
$eff-cond$	-	Purely conductive effective quantity
g	-	Gas related quantity
i	-	Iteration number
$init$	-	Initial quantity
lim	-	Maximum allowed quantity
max	-	Maximum quantity
max_serv	-	Maximum service quantity
n	-	Unit cell layer designations A, B, C, D
o	-	Quantity in the absence of a pressure difference

- r* - Radiation based quantity
- room* - Room conditions based quantity
- s* - Solid related quantity

1. INTRODUCTION

The use of (astronautic) space offers new and attractive opportunities for global coverage, quick response and reduced risk to the U.S. military forces. For example, the use of space can give the U.S. military a capacity to strike from space a variety of targets by non-nuclear means. Such strikes could be taken promptly, on demand, with a high precision and with a high flexibility relative to the nature of targets (e.g. hard and deeply buried targets, mobile targets, etc.). The Common Aero Vehicle (CAV) is a concept for aerodynamically designed un-powered re-entry vehicles with maneuvering capabilities for increased accuracy and range that would enable effective deployment of the desired submunitions. Currently, the CAV concept is being viewed as a potential way of exploiting the aforementioned advantages of the space. To meet the previously mentioned requirements for target flexibility, the CAVs are envisioned to carry a few small smart bombs, a few powered autonomous attack munitions, a hard and a deeply buried target penetrator, and other special weapon payloads. The CAVs are planned to be delivered from either a future military space plane or from conventional ballistic missiles [1, 2].

The overarching goal of the CAV development is to be cost competitive with cruise missiles and other precision guided munitions. The majority of estimates place the cost of a single CAV at about 1.5 million dollars. In order to meet this objective, the design of CAVs must be kept as simple as possible. One of the major simplifications of a CAV design relative to that in a standard Shuttle orbiter, is the potential elimination of the altitude control system. The Shuttle orbiter uses this system during re-entry all the way down to Mach number 2.0 before switching to all aerodynamic flight controls. The use of this system is required because the Shuttle re-enters the atmosphere at a large (up to 45 degree) angle of attack in order to spread the heat over the entire windward surface of the vehicle and, hence, in order to protect its reusable thermal protection system (TPS). In the case of CAVs, the thermal protection system does not need to be reusable and the concern is only that its erosion does not compromise the aerodynamic performance of the vehicle. Consequently, the CAVs are expected to fly under low values of the angle of attack, i.e. under the conditions which maximize the lift-drag ratio and give rise to the highest possible downrange and crossrange distances [1, 2].

The current thermal protection system (TPS) technology imposes the most significant limitation on the attainable CAV performance. It is generally agreed that if a CAV is allowed to operate for about 3,000 seconds under severe aerothermal conditions, the performance of the CAV would be practically unconstrained relative to what trajectory it could follow. Under such circumstances, impressive crossrange and downrange distances of 3,000 and 15,000 nautical miles, respectively are predicted when a CAV re-enters the earth's atmosphere from an orbit. Unfortunately, the current TPS technology would allow the CAVs to be flown only for approximately 800 seconds in the high heat rate aerothermal conditions and, hence, the CAV has to be flown much more conservatively in order for the TPS to survive [1, 2].

If a CAV were built today, the critical aerodynamic surfaces such as the nose and the movable control surfaces would be made out of carbon-carbon composite in order to ensure a minimum degree of erosion. The remaining surfaces would be made out of ablative materials such as carbon phenolics. With these choices of materials, the TPS is estimated to take between 50-60% of the CAV aeroshell total weight. This is a relatively high number and various efforts are being made to design, develop and fabricate materials which can reduce the weight of the TPS while enabling the CAV flight time to be placed near the target of 3,000 seconds. It should be noted that the present TPS technology can provide CAV flight times of only up to 800 s, with maximum attainable crossrange and downrange distances of only about 900 and 2,000 nautical miles, respectively. These seriously reduce the operational flexibility of the CAVs, leaving the possibility that some targets may be difficult to reach.

The objective of the present work is to carry out a critical assessment of CFOAM[®], a carbon-based foam material as a candidate material for the future CAV thermal protection needs. A simple schematic of the CAV including dimensions, main components and three characteristic locations at the vehicle surface (STA-000, STA-051 and STA-255) are displayed in Fig.1 [1]. The main functional objective of the TPS system is to ensure that the interior of the CAV is not subjected to temperatures exceeding a maximum allowed temperature (typically set to 430 K for an aluminum-based CAV structural frame) and that the TPS ensures the structural integrity of the vehicle without compromising its aerodynamic performance.

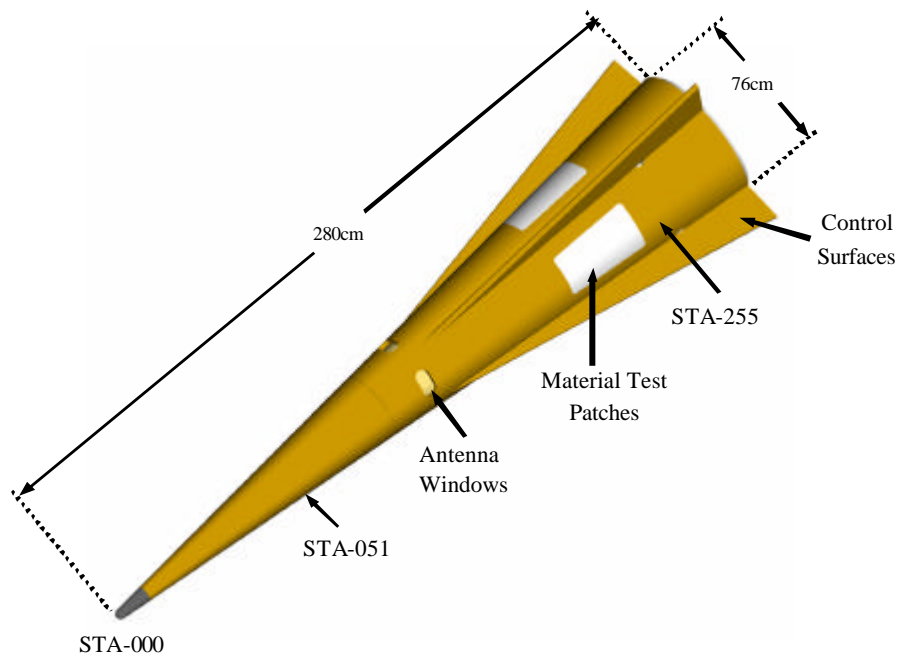


Fig.1. A schematic of the Common Aero Vehicle (CAV), and along with its typical dimensions and three characteristic locations at which the suitability of CFOAM[®] for TPS applications is examined.

Due to their light weight and potential tailorability of their physical and mechanical properties over a wide range, foam-like materials based on metals, ceramics, polymers and their mixtures have received over the last several years a great deal of attention [e.g. 3]. Recently, a new carbon-based foam called CFOAM[®] was developed which possesses an excellent combination of tailorable thermal, mechanical and physical properties. For example, electrical conductivity of CFOAM[®] can be varied over seven orders of magnitude. This material does not produce off-gases at elevated temperatures and does not support ignition and, hence, it possesses a high fire resistance. In addition, CFOAM[®] has excellent sound-absorbing capabilities [4].

CFOAM[®] is produced by Touchstone Research Laboratory, Ltd. from high sulfur bituminous coal using a proprietary technology and it is available in two principal microstructures: (a) An open-cell reticulated microstructure consisting of a ligament network and (b) a closed-cell (cellular) microstructure consisting of thin-wall spherical cells. The two forms of CFOAM[®] are generally referred to as CFOAM-17[®] and CFOAM-25[®], respectively, where the numbers 17 and 25 pertain to the material density in pounds per cubic foot. A summary of typical room-temperature properties of CFOAM-17[®] and CFOAM-25[®] is given in Table 1. In the present work, only CFOAM-17[®] will be analyzed. Currently, CFOAM-17[®] is being considered for use in thermal-insulation and structural applications. Specifically, CFOAM-17[®] is presently being studied as a candidate insulation filling material in metallic thermal protection system (TPS) panels and for backside insulation of the carbon-carbon TPS sections of the nose cap and the leading edges on the future space vehicles.

Recently, a comprehensive experimental investigation was carried out of the thermo-mechanical properties of CFOAM-17[®] as a function of test temperature (up to 2300K) and as a function of temperature of its graphitization heat treatment [5]. The results obtained show that only CFOAM-17[®] graphitized at temperatures in excess of 2300K, is microstructurally stable during experimental measurements of its thermo-mechanical properties. For the CFOAM-17[®] heat treated at a lower temperature, the graphitization process continues during testing leading to an anomalous effect of test temperature on material properties (e.g. a negative thermal expansion coefficient, a substantial increase in thermal conductivity of the material with an increase in test temperature, etc.). The conclusion reached in this experimental investigation was that CFOAM-17[®] should be given a graphitization heat treatment at a temperature in excess of 2300K in order for it to be suitable for the TPS insulation applications. Consequently, only the CFOAM-17[®] given such a graphitization heat treatment will be analyzed in the present work.

To better understand the experimentally measured thermal properties of CFOAM-17[®] and their variation with test temperature [5], a simple model was proposed in our recent work [6]. The model treats the transfer of heat through a foam-like material like CFOAM-17[®] as a combined effect of conduction through the solid phase of the foam, conduction through the gas residing within the pores of the foam and radiation of the foam ligament/cell surfaces. The model accounts for the fact that relative contributions of these three modes of heat transfer vary as a function of the local conditions of temperature and pressure. To enhance this model in order to include the effect of foam microstructure, a simple periodic tetrakaidecahedrons-based microstructure for CFOAM-17[®] is assumed in the present work.

The organization of the paper is as follows: A brief description of the effective thermal conductivity model developed in the present paper is presented in Section 2.1.

Table 1. Typical Values of the Mechanical and Physical Properties of CFOAM-17[®] Used in the Present Work and for CFOAM-25[®] [2].

Property	Test Method Used	Unit	Value		Comments
			CFOAM -17 [®]	CFOAM -25 [®]	
Nominal Density	ASTM D 1622	kg/m ³	270	400	
Compressive Strength	ASTM C 365	MPa	>4.8	>15	
Compressive Modulus	ASTM C 365	MPa	200	830	
Tensile Strength	ASTM C 297	MPa	>1.7	>3.5	
Tensile Modulus	ASTM C 297	MPa	200	830	
Shear Strength	D5379/5379M	MPa	1.4	2.1	
Coefficient of Thermal Expansion	ASTM E 228	ppm/K	5.0	5.8	
Thermal Conductivity	ASTM E 1225	W/m-K	0.25 to 25		Tailorable
Maximum Service Temperature	N/A	K	3300 in Inert Atmosphere		
Electrical Resistivity	ASTMD 4496	Ohm-cm	10 ⁰² to 10 ⁺⁰⁷		Taylorable
Fire Resistance	ISO 1182, ASTM E 1354, ASTM E 1515, MIL-STD-1623 Coast Guard IMO FTP Code Part I and III	N/A	Pass		Results indicate CFOAM [®] will pass all key fire tests including: radiant panel, smoke generation, toxicity, cone calorimeter, fire resistance, and room corner tests.

The computational procedure used to determine the minimum CFOAM-17[®] insulation thickness and to judge the suitability of CFOAM-17[®] in the TPS of future CAVs is overviewed in Section 2.2. The results obtained in the present work are presented and discussed in Section 3. The main conclusions resulting from the present work are summarized in Section 4.

2. PROCEDURE

2.1. Effective Thermal Conductivity Model

As previously stated CFOAM-17[®] has an open-cell structure and, hence, the heat transfer through it can involve conduction (through both the solid phase and the gas phase), convection within the gas phase and radiation between foam ligament surfaces. Since the cell structure in a foam material like CFOAM-17[®] interferes with a large-scale motion of the gas phase, convection is generally not considered as an important mode for heat transfer through a foam-like material. Consequently, the heat transfer through CFOAM-17[®] is considered to take place either by solid-phase conduction, gas-phase conduction or by radiation. To determine the effective thermal conductivity of CFOAM-17[®], which is defined as a sum of the conduction and radiative thermal conductivities, the models recently proposed by Boomsma and Poulidakos [7] and Zhao et al. [8] are combined. In the following, a brief description is given of these two models.

2.1.1 Purely-conductive Effective Thermal Conductivity

Boomsma and Poulidakos [7] recently developed a geometrical model for purely conductive effective thermal conductivity of saturated porous foams. The term “*purely conductive*” is used to denote that the model of Boomsma and Poulidakos [7] considers only the conduction heat transfer through an open-cell foam-like material. The model is based on an idealized three-dimensional foam-cell geometry which consists of space-filling tetrakaidecahedrons, Fig.2. This specific geometry is characterized as the space-filling cell shape which minimizes the surface area for the given volume of the solid phase and a given value of the ligament diameter-to-length ratio. The ligaments are of circular cross-section and they are attached to each other by cubic nodes. In the real microstructure of CFOAM-17[®], the nodal points contain smoothly distributed excess material which in the model is approximated by a cubic shape, Fig.2.

Due to the inherent symmetry of the tetrakaidecahedrons, a box-shape unit cell (represented by dashed lines in Fig.2) which represents one sixteenth of a tetrakaidecahedron can be used to analyze the problem of heat conduction through a foam material with the simplified cell structure. The edge lengths of the unit cells are $L\sqrt{2}/2$, $L\sqrt{2}$ and $L\sqrt{2}$, where L is the distance between the node centers in the tetrakaidecahedrons.

As indicated in Fig.3 (a), the unit cell can be broken down into four distinct vertical layers designated as A , B , C and D . The relative volume fractions of the solid and the gas phases are fixed in each layer. The thermal conductivity of each layer $n=A, B, C$ or

D is then calculated by volume averaging of thermal conductivities of the solid and gas phases as:

$$k_n = \frac{V_{n,s}k_s + (V_n - V_{n,s})k_g}{V_n} \quad (1)$$

where subscripts s and g are used to denote the solid and gas phases, respectively and V_n is the volume of the particular phase/layer.

The purely-conductive effective thermal conductivity, $k_{eff-cond}$, through the unit cell is then calculated by considering the heat flow through a series of the four layers as:

$$k_{eff-cond} = \frac{L_A + L_B + L_C + L_D}{(L_A/k_A) + (L_B/k_B) + (L_C/k_C) + (L_D/k_D)} \quad (2)$$

where L_n ($n=A, B, C, D$) are the thicknesses of the four layers and are given in Fig.2(a).

Eq. (2) can be recasted in the following form:

$$k_{eff-cond} = \frac{\sqrt{2}}{2(R_A + R_B + R_C + R_D)} \quad (3)$$

where the four simplifying quantities R_A , R_B , R_C and R_D are defined as:

$$R_A = \frac{4d}{(2e^2 + pd(1-e))k_s + (4 - 2e^2 - pd(1-e))k_g} \quad (4)$$

$$R_B = \frac{(e-2d)^2}{(e-2d)e^2k_s + (2e-4d-(e-2d)e^2)k_g} \quad (5)$$

$$R_C = \frac{(\sqrt{2}-2e)^2}{2pd^2(1-2e\sqrt{2})k_s + 2(\sqrt{2}-2e-pd^2(1-2e\sqrt{2}))k_g} \quad (6)$$

$$R_D = \frac{2e}{e^2k_s + (4-e^2)k_g} \quad (7)$$

where the dimensionless node length, e , is given by:

$$e = \frac{r}{L} \quad (8)$$

with r being the node length, and the dimensionless foam ligament radius, d , is defined as:

$$d = \frac{a}{L} \quad (9)$$

with a being foam ligament radius.

The foam porosity, ϵ , is related to d and e through the following relation:

$$\epsilon = 1 - \frac{\sqrt{2}}{2} \left(de^2 + \frac{1}{2}pd^2(1-e) + \left(\frac{1}{2}e-d \right) e^2 + pd^2(1-2e\sqrt{2}) + \frac{1}{4}e^3 \right) \quad (10)$$

Likewise d is related to e and ϵ through the following relation:

$$d = \sqrt{\frac{\sqrt{2}(2 - (5/8)e^3\sqrt{2} - 2\epsilon)}{p(3 - 4e\sqrt{2} - e)}} \quad (11)$$

An examination of Eqs.(1-11) reveals that in order to compute the purely-conductive effective thermal conductivity, the following input parameters are required: thermal conductivities of the solid phase, k_s , thermal conductivity of the gas phase, k_g , foam porosity, ϵ , and the dimensionless cubic node length e . This may suggest that purely-conductive effective thermal conductivity does not depend on the absolute scale of the foam structure. However, as will be shown below, thermal conductivity of the gas maybe affected by the ratio of the molecular mean free path and the cell size and, thus, the absolute scale of the cell structure becomes important.

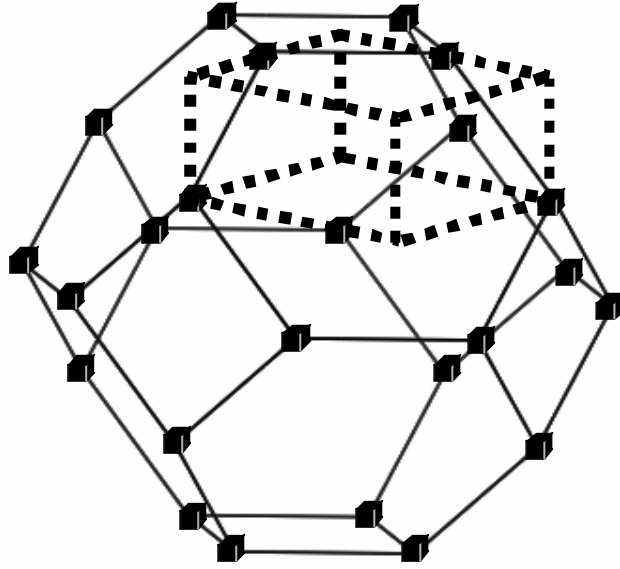


Fig.2. A schematic of tetrakaidecahedron model used to present the open-cell microstructure of CFOAM[®] consisting of cylindrical ligaments and cubic nodal points. The unit cell used in the calculations of conduction only thermal conductivity is shown using dashed lines.

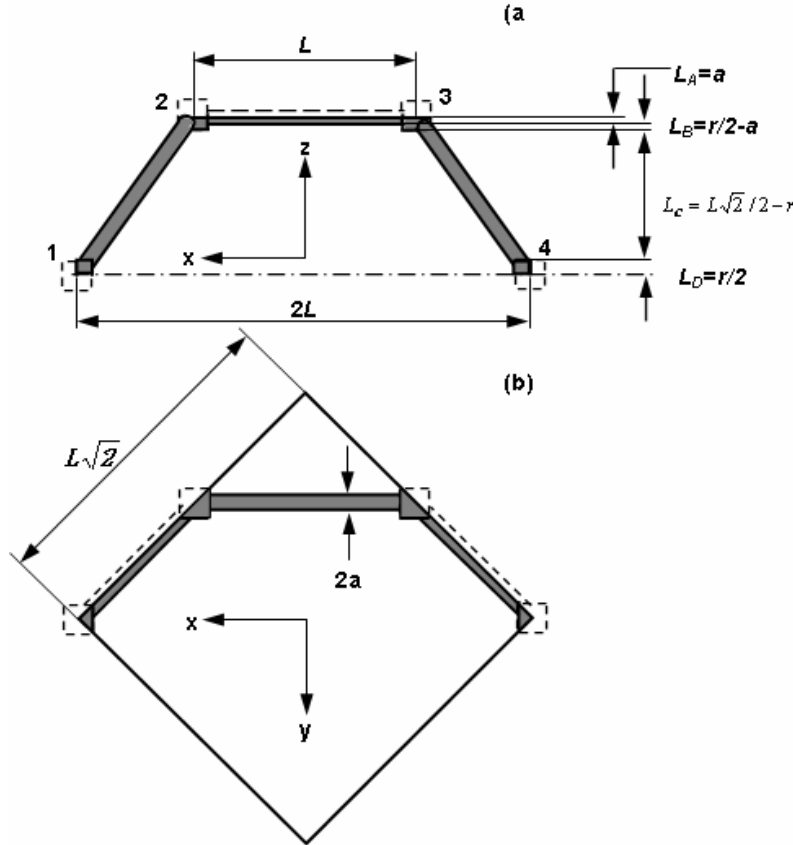


Fig.3. (a) Side view and (b) top view of the unit cell shown in Fig.2. Shaded regions denote the portions of ligament and nodes which fall into the unit cell of interest.

2.1.2 Radiation Thermal Conductivity

As shown in our recent work [6], the contribution of radiation to the heat transfer through a foam-like material can be modeled by simultaneously solving the energy conservation equation and a radiation heat transfer equation. However, the complex nature of the open-cell foam microstructure makes the analysis of heat radiation through a foam-like material quite challenging and time consuming. To overcome this problem, a foam-like material is typically simplified as a semi-transparent isotropic effective medium, and the radiative heat transfer is modeled using either a two-flux approximation [e.g. 9, 10] or a diffusion approximation [e.g. 11, 12]. Since the latter of these two approximations, is generally found to provide a better physical understanding of thermal radiation in the foam-like materials, it is employed in the present work. In addition, carbon-based foams like CFOAM-17[®] are, in general, optically sufficiently thick so that the approximation that radiation heat transfer is of a diffusive nature is well justified in these materials. In other words, when the optical thickness is sufficiently large, the local radiation heat transfer is mainly controlled by the local temperature

gradient. Under such conditions, one can define a radiation-based thermal conductivity, k_r . Within the effective medium approximation, the radiative thermal conductivity is defined by the Rosseland equation [13] as:

$$k_r = \frac{16hsT^3}{3K_R} \quad (12)$$

where h is the emissivity, $s = 5.669 \times 10^{-8} \text{ W/m}^2\text{K}^4$ is the Stefan-Boltzmann constant, and K_R is the Rosseland mean extinction coefficient which is defined as:

$$\frac{1}{K_R} = \int_0^\infty \frac{1}{K_I} \frac{dE_{bl}(T, I)}{dE_b(T)} dI \quad (13)$$

where K_I is the spectral extinction coefficient while the spectral E_{bl} and the total E_b emissive powers of a blackbody are respectively given as:

$$E_{bl}(T, I) = \frac{C_1 I^{-5}}{e^{C_2/I} - 1} \quad (14)$$

and

$$E_b(T) = sT^4 \quad (15)$$

Eq. (14) is based on the Planck's quantum concept for electromagnetic energy with $C_1 = 3.743 \times 10^{-16} \text{ Wm}^2$ and $C_2 = 1.4387 \times 10^2 \text{ mK}$, and I is the photon wave length.

Following Zhao et al. [8], the spectral extinction coefficient is defined as:

$$K_I = C \frac{(1 - \epsilon)^n}{a} \quad (16)$$

where the constant C and n are respectively set to 2.5 and 1.0 [8].

Substitution of Eqs.(16), (14) and (15) into Eq.(13), integration of the resulting equation to get K_R as a function of temperature and the substitution of this relation into Eq.(12) yields the variation of the radiation thermal conductivity, k_g , as a function of temperature.

2.1.3 Effective Thermal Conductivity

Since the transfer of heat through a foam-like material, takes place in parallel by conduction and radiation, the total effective thermal conductivity, k_{eff} , is define as a sum of the purely conductive effective thermal conductivity $k_{eff-cond}$, and the radiative thermal conductivity, k_g , as:

$$k_{eff} = k_{eff-cond} + k_r \quad (17)$$

2.1.4 Thermal Conductivity of Gas

While thermal conductivity of the bulk solid phase generally shows weak temperature and pressure dependences, thermal conductivity of the gas is typically a very sensitive function of both temperature and pressure. Following Daryabeigi and co-workers [14-15], thermal conductivity of the gas phase is defined as:

$$k_g = \frac{k_{g,o}}{F + ? \cdot 2 \frac{2-a}{a} \frac{2 \cdot g}{g+1} \frac{1}{Pr} Kn} \quad (18)$$

where $k_{g,o}$ is temperature-dependent thermal conductivity of the gas phase at the atmospheric pressure, a is a thermal accommodation factor (a fraction of gas molecules which come into thermal equilibrium with the solid phase during collision with the surface of the solid phase), g a constant-pressure over constant-volume specific heats ratio, Pr the Prandtl number, and Kn the Knudsen number. Parameters F and $?$ depend on the gas-phase regime, i.e. on the magnitude of the Knudsen number: For $Kn \leq 0.01$ (i.e. for the continuum gas-phase regime), $F = 1$ and $? = 0$, and thus $k_g = k_{g,o}$; for $0.01 \leq Kn \leq 10$ (i.e. for the transition regime), $F = 1$ and $? = 1$; and for $Kn \geq 10$ (i.e. for the free molecular regime), $F = 0$ and $? = 1$.

The Knudsen number is defined as:

$$Kn = \frac{l}{d} \quad (19)$$

where the gas molecular mean field path, l , is defined as:

$$l = \frac{K_B T}{\sqrt{2} p P d_g^2} \quad (20)$$

and the characteristic length scale for gas molecules in a reticulated porous medium, d , is defined as [14]:

$$d = \frac{pa}{4(1-e)} \quad (21)$$

where K_B is the Boltzmann's constant, P the pressure, d_g the gas collision diameter, and a the foam ligament radius.

A list of thermo-physical parameters for the solid phase in CFOAM-17[®] and for the gas (air) used in the present work is given in Table 2. A detailed description of the procedure used to access the quantities listed in Table 2 is presented in our recent work [6].

2.2. CFOAM-17[®] Thickness Sizing Procedure

As explained in Section 1, the main objective of the present work is to examine the suitability of CFOAM-17[®] for use in TPS insulation applications in future CAVs. One of the key parameters controlling the suitability of CFOAM-17[®] in such applications is the minimum insulation thickness required to ensure that the temperature of the underlying structure does not at any moment during re-entry, exceed a maximum allowed temperature, T_{lim} . When the CAV structure is constructed using aluminum or its alloys, the maximum allowable temperature is generally set to 430K. This value of T_{lim} , will be used in the present work.

Table 2. Thermo -physical Properties of CFOAM-17[®] and Nitrogen Gas Used in the Present work.

Property	Symbol	Unit	Value	Equation Where First Used
CFOAM [®] Density	\mathbf{r}	kg/m ³	Eq.(23)	Eq. (22)
CFOAM [®] Specific Heat	C_p	J/kg-K	Fig.4	Eq. (22)
CFOAM [®] Effective Thermal Conductivity at Room Temperature	k_{eff}	W/m-K	Fig.7	Eq. (17)
CFOAM [®] Emissivity	\mathbf{h}	N/A	0.85	Eq. (12)
CFOAM [®] Porosity	e	N/A	Eq.(24)	Eq. (10)
Collision Diameter for Nitrogen Gas	d_g	m	3.74×10^{-10}	Eq. (20)
Specific Heat Ratio for Nitrogen Gas	?	N/A	1.4	Eq. (18)
Thermal Accommodation Factor for Nitrogen Gas	a	N/A	1	Eq. (18)
1atm_Pressure Thermal Conductivity of Nitrogen Gas	$k_{g,o}$	W/m-K	$1.3 \times 10^{-11} T^3 - 4.5 \times 10^{-8} T^2 + 9.4 \times 10^{-5} T + 0.0014$	Eq. (18)
Prandtl Number of Nitrogen Gas	P_r	N/A	$-2.1 \times 10^{-10} T^3 + 5.5 \times 10^{-7} T^2 - 0.00038 T + 0.79$	Eq. (18)

To determine the minimum required CFOAM-17[®] thickness at the three locations indicated in Fig.1, a one dimensional heat transfer model is developed and applied at each of the locations. The model involves a single one dimensional energy conservation equation in the form:

$$\mathbf{r}(P_{dyn} - P_{atm})C_p(T)\frac{\partial T}{\partial t} = k_{eff}(T, P_{atm}, P_{dyn} - P_{atm})\frac{\partial^2 T}{\partial x^2} \quad (22)$$

where T is the temperature, t the time, x the spatial coordinate, the temperature-dependent constant-pressure specific heat, C_p , is taken from our previous work [5], and displayed in Fig.4, and the material density is assumed to depend on the difference between the (aero)dynamic pressure, P_{dyn} , and the atmospheric pressure, P_{atm} , according to the following relation:

$$\mathbf{r} = \frac{E\mathbf{r}_0}{E - (P_{dyn} - P_{atm})} \quad (23)$$

where E is the compressive bulk modulus.

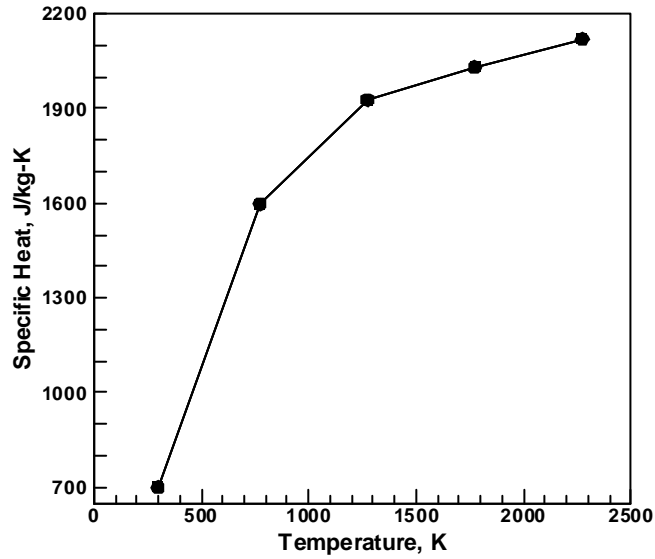


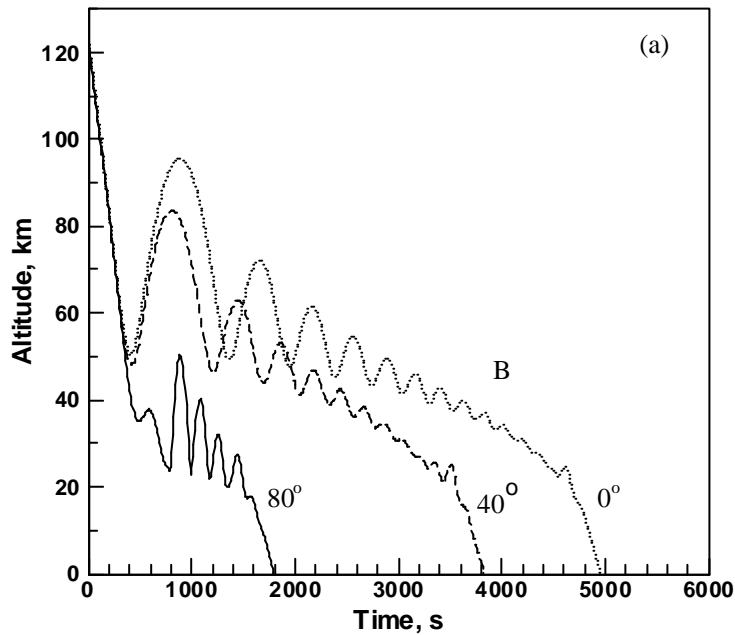
Fig.4. The effect of test temperature on the heat capacity in CFOAM-17[®].

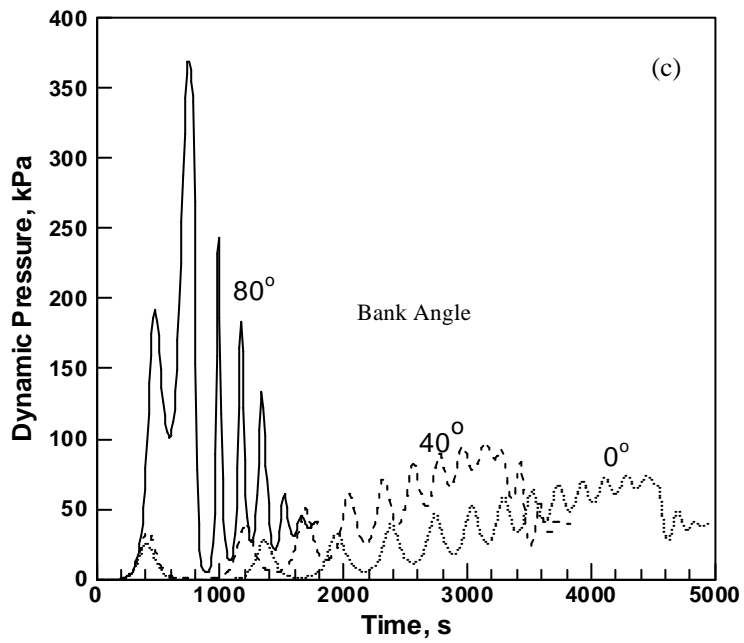
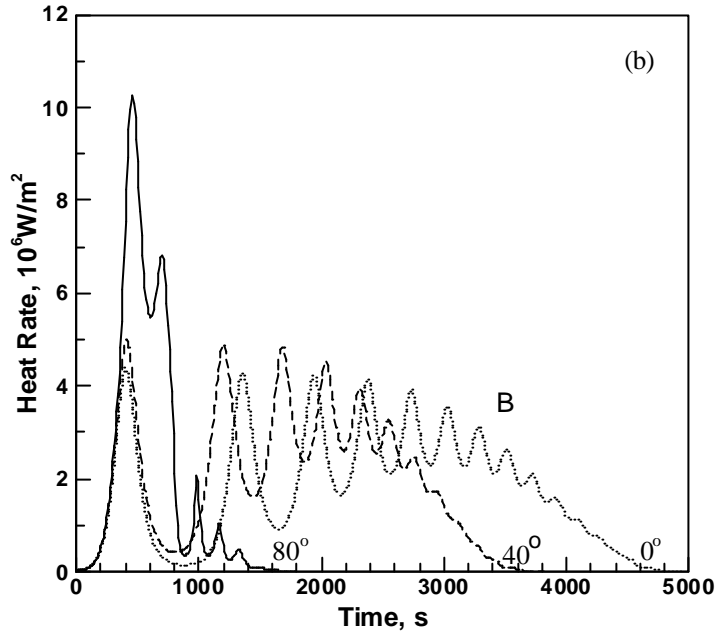
The effective thermal conductivity, k_{eff} , derived in the previous section is taken to depend not only on temperature and pressure but also on the pressure difference ($P_{dyn} - P_{atm}$) since such a difference affects the effective CFOAM-17[®] porosity through the following relation:

$$\mathbf{e} = 1 - \frac{E(1 - \mathbf{e}_0)}{E - (P_{dyn} - P_{atm})} \quad (24)$$

A subscript o is used in Eqs. (23) and (24) to denote the material density and porosity in the absence of a pressure difference.

The trajectory data for the variation of altitude, heat rate, dynamic pressure and atmospheric pressure for three typical bank angles for a CAV are shown in Figs 5(a)-(d), respectively [16]. These results correspond to the following CAV re-entry conditions: the initial velocity 7.315 km/s at the initial altitude of 122km, the re-entry angle -1.5deg , the initial angle of attack 10deg followed by an angle of attack of 15deg at a CAV velocity corresponding to Mach number 5 and the maximum lift-to-drag ratio 2.4. These data are used in conjunction with Eq. (22) in the CFOAM-17[®] thickness sizing procedure discussed below. The heat rate data, Fig.5 (b), and the dynamic pressure data, Fig.5(c), pertain to the stagnation point (STA-000) of the CAV. While complete heat rate and dynamic pressure trajectories for the other two locations of the CAV were not given in Ref. [16], they are postulated to scale with the given maximum values of the heat rate at these locations. The resulting scaling factors (defined as the ratio of the maximum heat rate at a given location and the maximum heat rate at the nose tip) used for the locations STA-051 and STA 055 are listed in Table 3.





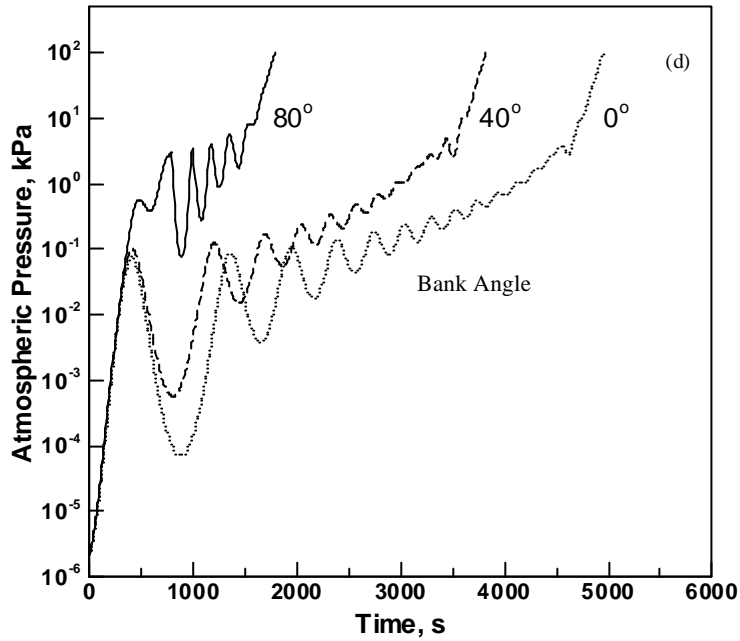


Fig.5. Typical trajectory data for a Common Aero Vehicle (CAV) for three values of the bank angle: (a) altitude vs. time; (b) heat rate vs. time; (c) dynamic pressure vs. time; (d) atmospheric pressure vs. time.

Table3. Maximum heat rates experienced by the CAV at three different locations relative to the CAV nose tip for both leeward and windward sides of the vehicle

Reference Location	Distance From Nose, cm	Heat Rate Ratio		Dynamic Pressure Ratio	
		Leeward Side	Windward Side	Leeward Side	Windward Side
STA-000	0.0	1.0	1.0	1.0	1.0
STA-051	50.8	0.0250	0.275	0.0250	0.275
STA-255	254.6	0.0167	0.130	0.0167	0.130

Eq. (22) is subjected to the following initial and boundary conditions:

$$T(x, t = 0) = T_{init} \quad (25)$$

$$q(x = h, t) = q_{aero}(t) - h_s (T^4(x = h, t) - T_{atm}^4(t)) \quad (26)$$

and

$$q(x=0, t) = 0 \quad (27)$$

where $x=h$ and $x=0$ correspond respectively to the outer and the inner surfaces of the CFOAM-17[®] insulation, q_{aero} denotes the aerodynamic heat rate whose time variation is given in Fig.5(b) and T_{atm} is the altitude-dependent atmospheric temperature. The adiabatic boundary condition at $x=0$ is assumed in order to obtain a conservative estimate for the minimal insulation thickness. In general, some heat losses are expected from the inner insulation surface which would reduce the temperature at this location. Such losses are ignored in the present work. The temperature of the CAV structure is assumed to be equal to the temperature at the inner surface of the insulation.

Variations of density and porosity of the CFOAM-17[®] insulation during a CAV flight are obtained by combining the dynamic pressure vs. time data (Fig.5(c)), the atmospheric pressure vs. time data (Fig.5(d)) with Eqs.(23) and (24), respectively.

Eq.(22) is solved using an iterative implicit finite difference method. A schematic of the one-dimensional model analyzed in the present work is shown in Fig.6. A standard mesh convergence analysis was conducted but the results of this analysis will not be presented here for brevity.

The CFOAM-17[®] thickness sizing procedure is carried out using the following steps:

- (a) An initial insulation thickness is assumed;
- (b) Eq.(22) is solved over the entire CAV flight trajectory and the maximum temperature at the inner surface of the insulation, T_{max} , recorded;
- (c) T_{max} is next compared with T_{lim} , using the following convergence criterion:

$$\left| \frac{T_{max} - T_{lim}}{T_{lim} - T_{room}} \right| < 0.001 \quad (28)$$

- (d) If the maximum structural temperature did not meet the convergence criterion given by Eq.(27), the insulation thickness, h , is resized according to the following equation:

$$h_{i+1} = h_i \left(1 + \frac{T_{max} - T_{lim}}{T_{lim} - T_{room}} \right) \quad (29)$$

where i is the iteration number. The procedure is repeated starting with step (b).

- (e) If the convergence criterion is met, the current insulation thickness is used as the final insulation thickness.

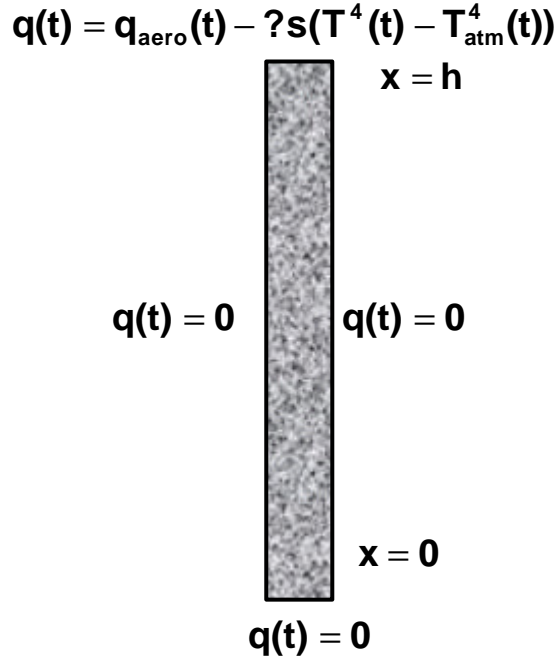


Fig.6. A schematic of the one-dimensional boundary value problem associated with heat transfer at a specific location of the TPS of a CAV.

3. RESULTS AND DISCUSSION

3.1. Effective Thermal Conductivity of CFOAM-17[®]

The model presented in Section 2.1 is utilized in the present section to compute the effective thermal conductivity of CFOAM-17[®] at various temperatures between the room temperature and 2273K. The results of these calculations are displayed in Fig.7. For comparison, the corresponding experimental data obtained in our recent work [5] are also displayed in Fig.7.

As explained in Section 2.1, the thermal conductivity of the solid phase in CFOAM-17[®] is selected in such a way that at the room temperature (and at 1atm atmospheric pressure) where gas-phase conduction and radiation play insignificant roles in the heat transfer through CFOAM-17[®], the computed and the experimental values for the effective thermal conductivity are identical. There are two sets of computational results displayed in Fig.7 which are respectively labeled as: “*Temperature Invariant*” and “*Temperature Dependent*”. These two sets of results pertain respectively: (a) to the case when the thermal conductivity of the solid phase is independent of temperature and (b) to the case when the thermal conductivity of the solid phase has the same relative temperature dependence as carbon as reported in Ref.[17], i.e. $k_s(T) = k_s(T_{\text{room}}) - a(T - T_{\text{room}}) = 13.746 - 0.002544(T - 298)$ W/m·K, where subscripts *s* and *room* are used to denote the solid phase and the room-temperature condition.

The results displayed in Fig.7 show that the two sets of computational results for the most part bracket the experimental data. It should be noted that, as discussed in Ref. [5], the experimental data at 773K were questionable and appear to be surprisingly high. Taking this into account it appears that the computational data labeled “*Temperature Dependent*” appear to give a somewhat better agreement with the experimental data. Hence, this version of the effective thermal conductivity model which accounts for the temperature dependence of the thermal conductivity of the solid phase is used in the remainder of this paper.

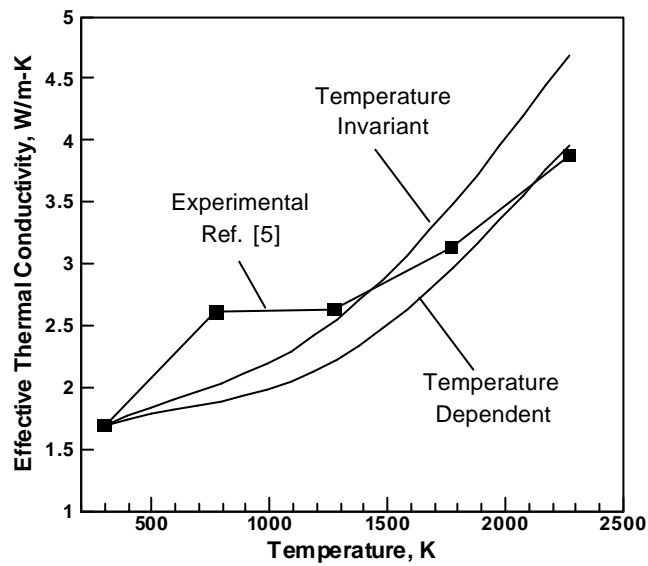


Fig.7. A comparison of the measured [5] and the computed effective thermal conductivities of CFOAM-17[®] at various temperatures above the room temperature. Please see text for an explanation of the curve levels.

3.2. Suitability and sizing of CFOAM-17[®] Insulation in CAV TPS

Applications

The CFOAM-17[®] insulation sizing procedure developed and presented in Section 2.2 is utilized in this section to identify the portions of the CAV's surface on which CFOAM-17[®] can be considered as a suitable TPS insulation material. As will be discussed below, CFOAM-17[®] can be considered as a suitable TPS insulation at a given location on the CAV surface only if its temperature during CAV re-entry never exceeds the local maximum allowable surface temperature for this material while its thickness does not exceed a maximum acceptable value. The term “*local*” is used to indicate that, as will be shown below, the maximum allowable service temperatures depend on the local value of the atmospheric pressure.

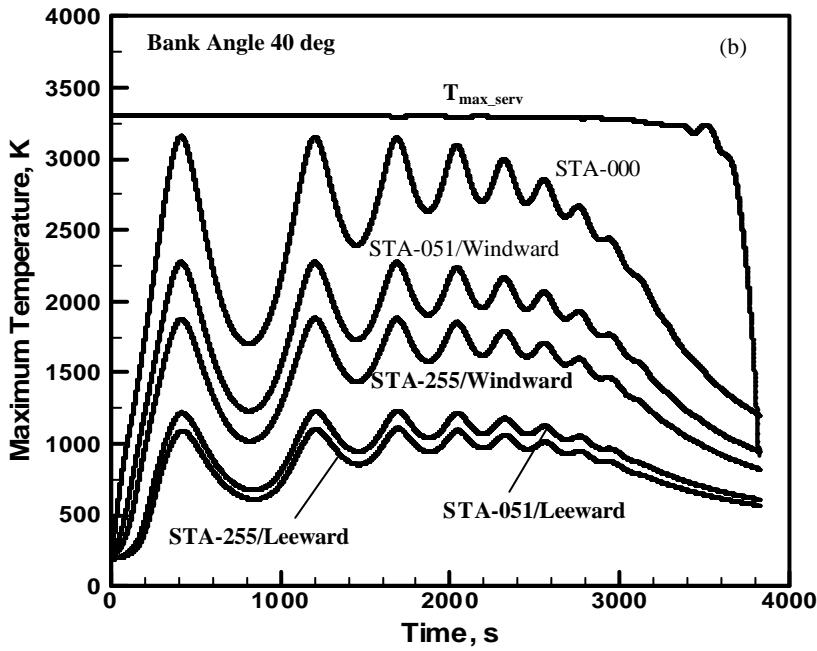
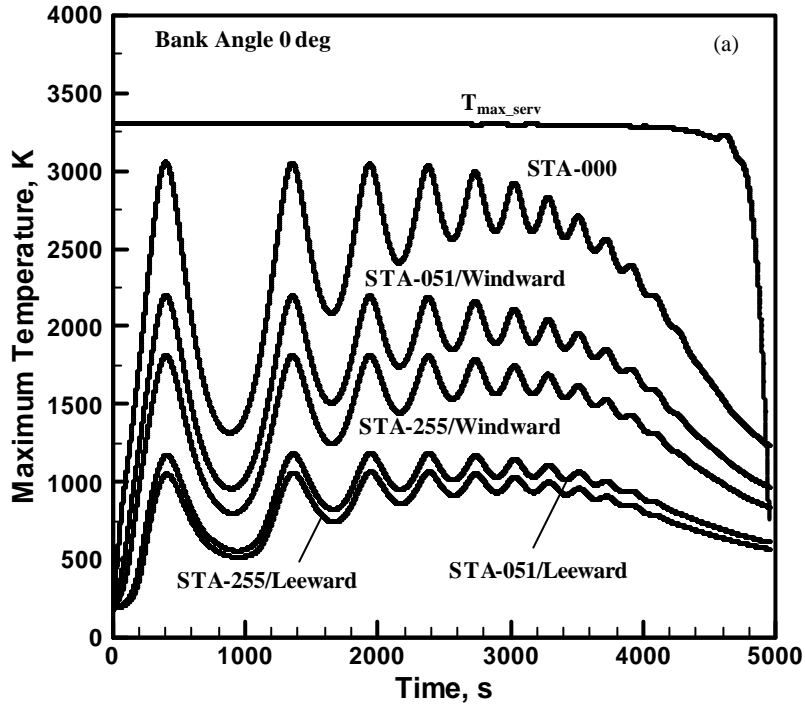
As indicated in Table 3, the maximum allowable service temperature for CFOAM-17[®] is 3300K in an inert atmosphere. This temperature is significantly lower in the presence of oxygen and, consequently, in air at 1 atm can be as low as 800K. For

CFOAM-17[®] to be a suitable TPS insulation material at a given CAV location, it is imperative that the temperature experienced by this material at that location does not exceed the local maximum allowable service temperature, T_{\max_sev} at any time. The maximum service temperature is defined as $T_{\max_sev}(K) = 3300 - 25P$ (where P is the local pressure in kPa) in the present work in order to account for the effect of partial pressure of oxygen in air on the thermal stability of CFOAM-17[®].

The temporal variations of the maximum allowable service temperature, T_{\max_sev} , for the CFOAM-17[®] insulation used as the TPS on a CAV are displayed in Figs 8(a)-(c) for the three typical values of the bank angle (0° , 40° and 80°), respectively. The curves corresponding to the maximum service temperature are denoted as T_{\max_sev} in Figs 8(a)-(c). These curves are obtained by combining the altitude vs. time data shown in Fig.5 (a) with the atmospheric pressure vs. time data displayed in Fig.5 (d) and with the above mentioned relation for T_{\max_sev} . Also shown in Figs 8(a)-(c), are the temporal evolutions of the maximum temperature within a CFOAM-17[®] insulation at different locations at the CAV surface. These results are denoted as STA-000, STA-051/Windward, etc. and correspond to the minimum insulation thickness needed to ensure that the temperature of the CAV structure does not exceed $T_{\lim} = 430K$ (discussed below).

The results displayed in Figs 8(a)-(c) show that regardless of the magnitude of the bank angle, the maximum temperature experienced by the CFOAM-17[®] insulation at the location STA-000 exceeds, at some portions of the re-entry trajectory, the maximum service temperature for this material. Hence, CFOAM-17[®] is not suitable for use in the TPS applications of the nose cone of a CAV. As far as the remaining locations at the CAV surface are concerned, the CFOAM-17[®] insulation may or may not be a suitable choice depending on the location, vehicle side (windward vs. leeward) and the magnitude of the bank angle. For instance, for the leeward side of the vehicle, CFOAM-17[®] at the locations STA-051 and STA-255 never experiences a temperature which exceeds the maximum allowable service temperature for this material for either of the three values of the bank angle. The same is true for STA-255 at the windward side of the vehicle but only for the magnitudes of the bank angle of 40° and 80° . As far as the location STA-051 at the windward side of the vehicle is concerned, only the re-entry conditions corresponding to the bank angle of 80° meet the functional requirement regarding the maximum insulation temperature never exceeding the local maximum allowable service temperature for CFOAM-17[®].

The results of the CFOAM-17[®] insulation thickness sizing procedure for a CAV's TPS system and the three values of the bank angle are displayed in Figs 9(a)-(c), respectively. As discussed above, the results displayed in Figs 8(a)-(c) show that the CFOAM-17[®] insulation is not suitable for the nose cone section of the CAV, since it experiences a maximum temperature during re-entry which exceeds a maximum allowable service temperature for this material. Nevertheless, the minimum thicknesses of a TPS insulation required to maintain the temperature of the CAV structure below 430K at the location on STA-000 for the three values of the bank angle are displayed in Figs 9(a)-(c) for completeness.



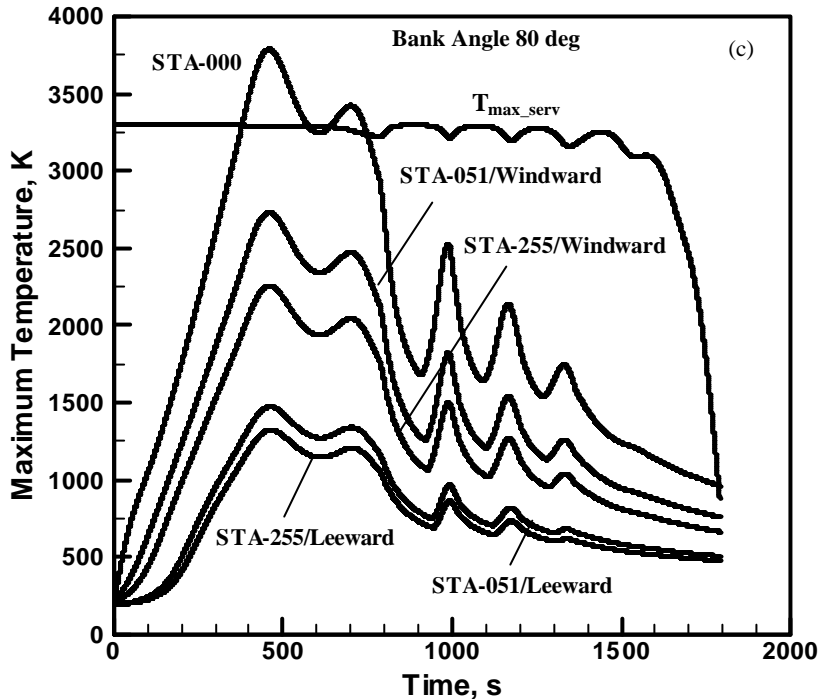


Fig.8. Temporal variations of the maximum allowable service temperature for CFOAM-17[®] during CAV re-entry and the maximum temperature experienced by the CFOAM-17[®] TPS insulation for the bank angle of: (a) 0°, (b) 40°, and (c) 80°.

It is generally preferred that the minimum required TPS insulation thickness be as small as possible since the insulation takes up the valuable space inside the CAV which is reserved for the storage of various weapons. As an example, consider that the limitation on the required insulation thickness is 15cm (approximately 6 inches). Using this particular criterion, the results displayed in Figs 9(a)-(c) suggest that CFOAM-17[®] is a suitable insulation material for the leeward side of a TPS on a CAV and for some portions of the windward side which are the furthest from the nose cone (e.g. location STA-255).

The results displayed in Figs 9(a)-(c) can be summarized as follows:

- (a) In general, CFOAM-17[®] can be used as a TPS insulation on the leeward side of a CAV regardless of the value of the bank angle.
- (b) For the windward side of the CAV, CFOAM-17[®] appears to be a reasonable choice for the TPS insulation material only for the largest value (80°) of the bank angle. It should be noted, however, that a large value of the bank angle can seriously compromise the CAV's operational capabilities. Consequently, the downrange is generally seriously reduced for the values of the bank angle of 40° and 80°, while at the larger values of the bank angle even the crossrange becomes compromised. Of course, if a slightly larger thickness limitation is deemed to be acceptable, then CFOAM-17[®] could be used for most of the windward side for all bank angles.

- (c) As pointed out earlier, CFOAM-17[®] should not be considered for TPS insulation application in the nose cone of a CAV.

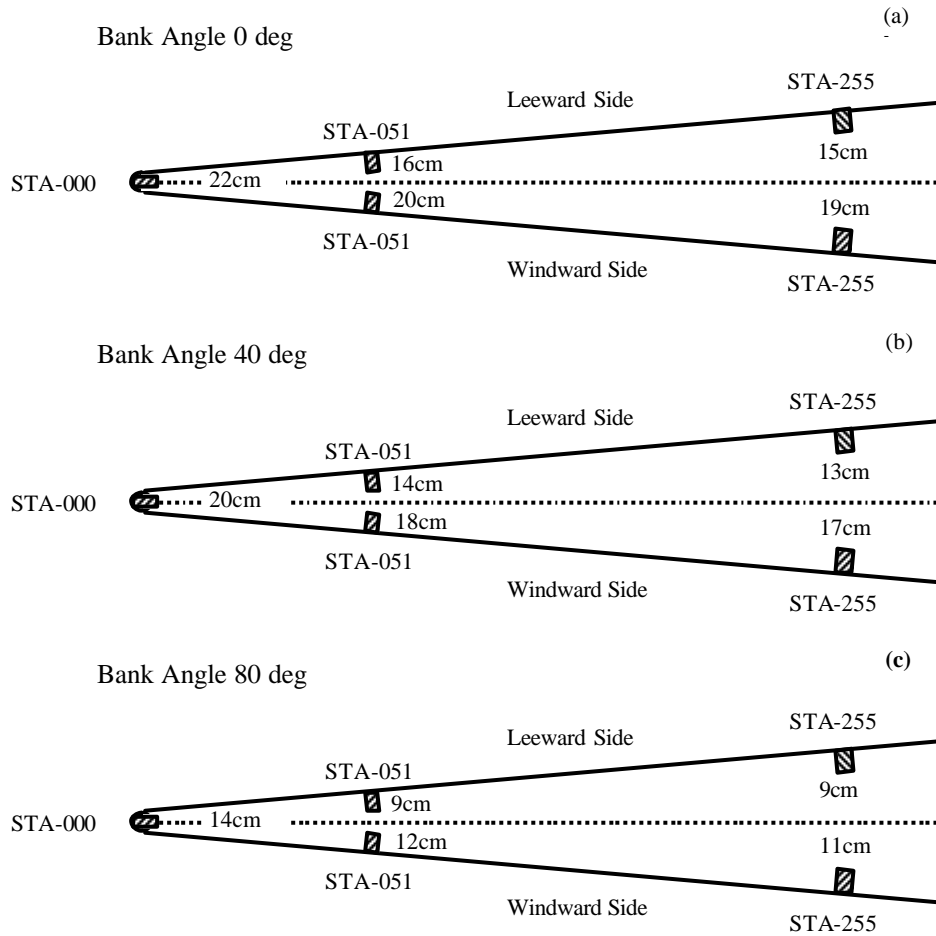


Fig.9. Minimum CFOAM-17[®] insulation thicknesses needed at different locations on the CAV surface to ensure that the maximum temperature of the CAV structure does not exceed 430K for the bank angle of: (a) 0°, (b) 40° and (c) 80°.

4. CONCLUSIONS

Based on the results obtained in the present work, the following main conclusions can be drawn:

1. The effective thermal conductivity of carbon-based, coal-derived foam-like materials such as CFOAM-17[®] at high temperatures can be successfully estimated by combining a pure-conduction thermal conductivity model which includes the details of the foam microstructure with a diffusion-based model for the radiation thermal conductivity.

2. When analyzing the suitability of an insulation material in thermal protection systems, at least two aspects of the material performance must be considered: (i) a requirement that the maximum temperature experienced by the insulation material should never exceed the maximum allowable surface temperature for that material in order not to compromise the aerodynamic performance of the space vehicle in question and (ii) a requirement that the minimum thickness of the material in question needed to ensure that the temperature of vehicle structure does not exceed the corresponding maximum allowable temperature should not take up too much of the vehicle interior space reserved for the payload.
3. For the expected design and the anticipated re-entry trajectories of a Common Aero Vehicle (CAV), CFOAM-17[®] has been found to be suitable for TPS insulation applications, primarily on the leeward side of the vehicle and at selected sections (those further away from the nose tip of the vehicle) on the windward side of the vehicle.

ACKNOWLEDGEMENTS

The material presented in this paper is based on work sponsored by the U.S. Air Force through Touchstone Research Laboratory, Ltd. The authors acknowledge valuable discussions with Professors Don Beasley, Richard Miller and Jay Ochterbeck of Clemson University.

REFERENCES

- [1]. T. H. Phillips, *A Common Aero Vehicle (CAV) Model, Description, and Employment Guide*, Schafer Corporation for AFRL and AFSPC, January 2003.
- [2]. *FALCON Force Application and Launch from CONUS Technology Demonstration*, Phase 1, Solicitation 03-XX, Defense Advantage Research Projects Agency, DARPA/TTO, June 2003.
- [3]. L. J. Gibson, and M. F. Ashby, *Cellular Solids*, Pergamon, New York, N.Y., 1988.
- [4]. D. R. Morgan, Thermal, Electrical and Structural Analysis of Graphite Foams, *MS Thesis*, University of North Texas, Denton, Texas, (2001).
- [5]. M. Grujicic, C. L. Zhao, S. B. Biggers, J. M. Kennedy and D. R. Morgan, Experimental Investigation and Modeling of Effective Thermal Conductivity and Its Temperature Dependence in A Carbon-Based Foam, *Journal of Materials: Design and Applications*, submitted for publication, June 2004.
- [6]. M. Grujicic, C. L. Zhao, S. B. Biggers, J. M. Kennedy and D. R. Morgan, Heat Transfer and Effective Thermal Conductivity Analyses In Carbon-based Foams for Use in Thermal Protection Systems, *Journal of Materials: Design and Applications*, submitted for publication, June 2004.
- [7]. K. Boomsma, and D. Poulikakos, On the Effective Thermal Conductivity of A Three-dimensionally structured Fluid-saturated Metal Foam, *International Journal of Heat and Mass Transfer*, 44(2001)827-836.
- [8]. C. Y. Zhao, T. J. Lu and H. P. Hodson, Thermal Radiation in Ultralight Metal Foams with Open Cells, *International Journal of Heat and Mass Transfer*, 47(2004)2927-2939.
- [9]. T. W. Tong, C. L. Tien, Radiative Transfer in Fibrous Insulations — Part I: Insulation Study, *J. Heat Transfer* 105(1) (1983)70–75.
- [10]. S. C. Lee, Effect of Fiber Orientation on Thermal Radiation in Fibrous Media, *Int. J. Heat Mass Transfer* 32(2) (1989)311–319.
- [11]. D. Baillis, M. Raynaud and J. F. Sacadura, Determination of Spectral Radiative Properties of Open Cell Foam: Model Validation, *J. Thermophys. Heat Transfer* 14 (2) (2000) 137–143.

- [12]. D. Baillis, M. Raynaud, and J. F. Sacadura, Spectral Radiative Properties of Open-Cell Foam Insulation, *J. Thermophys. Heat Transfer* 13(3) (1999)292–298.
- [13]. H. C. Hottel, A. F. Sarofim, *Radiative Transfer*, McGraw-Hill Book Company, 1967.
- [14]. D. Sullins and K. Daryabeigi, Effective Thermal Conductivity of High Porosity Open Cell Nickel Foam, *AIAA 2001-2819, 35th AIAA Thermophysics Conference*.
- [15]. K. Daryabeigi, Thermal Analysis and Design of Multi-layer Insulation for Re-entry Aerodynamic Heating, *AIAA 2001-2834, 35th AIAA Thermophysics Conference*.
- [16]. Williams, *Re-Entry Structures Experiment Flight Environment and Ground Test Information*, Flight Test Lead Space Vehicles Directorate Air Force Research Laboratory, June 2004.
- [17]. D. Doermann, J. F. Sacadura, Heat Transfer in Open Cell Foam Insulation, *Journal of Heat Transfer*, 118(1996)88-93.